Discovery of spectral variation in the optical counterpart of IRAS 01005+7910

By: V. G. Klochkova, M. V. Yushkin, A. S. Miroshnichenko, V. E. Panchuk, and K. S. Bjorkman

V. G. Klochkova, M. V. Yushkin, A. S. Miroshnichenko, V. E. Panchuk, and K. S. Bjorkman (2002) *A & AS.* **392**, 143-150. Discovery of spectral variation in the optical counterpart of IRAS 01005+7910.

Abstract:

We present a study of the high-resolution spectroscopic data for the proto-planetary nebula candidate IRAS 01005+7910. For the first time a careful spectral line identification is carried out, and a significant variability of the optical spectrum is detected. We found absorption lines of C II/III, N II, O II, Al III, Si III, and Mg II (λ4481 Å), as well as emission lines of Si II and [Fe II]. Both absorption and emission components are present in the Balmer lines, Na I resonance $D_{1,2}$ lines, He I, and Fe III lines. The He I line profiles vary from straight to inverse P Cyg-type on a timescale of days to months. The resonance Na I lines show 5 absorption components at a resolution of R = 60000. Additionally, the Na I D_2 line exhibits a variable emission component with a width comparable to that of the Balmer line emission components. Using the model atmospheres method within the LTE-approximation, the effective temperature ($T_{\rm eff}$ ~ 21500 K), the metallicity [Fe/H]⊙ = - 0.31, and the ratio C/O > 1 is reported. Finally, we suggest that IRAS 01005+7910 is a carbon-rich post-AGB star with a luminosity log(L/L⊙) = 3.6 at a distance about 3 kpc.

Key words: stars: evolution —– stars: AGB and post-AGB —– stars: emission-line – stars: individual: IRAS 01005+7910 – techniques: spectroscopic

Article:

1. Introduction

Proto-planetary nebulae (PPNe) are post-AGB objects evolving toward the Planetary Nebula (PN) stage with increasing effective temperatures ($T_{\rm eff}$) and almost constant luminosities (e.g. Blöcker 1995). They span a range of spectral types between *B* and *G* and are surrounded by a significant amount of circumstellar dust, thanks to which many such sources were detected by the IRAS satellite (Parthasarathy & Pottasch 1989). Follow-up observations showed that PPNe, especially those of early spectral types, exhibit variable emission-line spectra (Parthasarathy et al. 2000). Spectroscopic studies are crucial for constraining PPNe masses through determination of the fundamental parameters and their evolutionary state with measurements of the chemical composition and mass loss rate. Spectroscopic monitoring programmes, which are still rare, are important for studies of physical processes in the objects' immediate vicinity and for detecting binary PPNe (Van Winckel et al. 1995), whose population recently began to grow as a result of such programmes (see Van Winckel 2001 for a review).

Here we present the first results obtained in the course of spectroscopic monitoring of a poorly-studied PPN candidate IRAS 01005+7910 (hereafter IRAS 01005) at the 6-m telescope of the Russian Academy of Sciences. The object is located far from the Galactic plane (b = 16°) and is identified with an 11-mag. peculiar star. Its IRAS colours are similar to those of PPNe, lying in the region v in the IRAS two-colour diagram of Van der Veen & Habing (1988). However, in contrast to most of the PPNe, maser emission from IRAS 01005 has been detected neither in ^{12}CO nor in OH bands (Likkel 1989; Likkel et al. 1991; Omont et al. 1993). According to a chronological sequence suggested by Lewis (1989), this result indicates that the object is very close to the PN stage. The IR spectrum of IRAS 01005 (Hrivnak et al. 2000) contains emission bands at 3.3, 6.2, 7.7, 8.6, 11.3, 26, and 30μm which are characteristic of carbon-rich PPNe. At the same time, IRAS 01005 does not show the famous emission at 21μm, whose presence is attributed to an excess of the s-process elements (Klochkova 1998; Decin et al. 1998).

So far only low-resolution spectra of IRAS 01005 have been published by Hu (2001), who classified the object as B2 Ie. This author also mentioned no changes in a P Cyg-type Hα line profile in his spectra, obtained 10 years apart. No photometric variations of the object have been reported.

2. Observations and data reduction

The observations were obtained at the 6-m telescope of the Special Astrophysical Observatory (SAO) of the Russian Academy of Sciences with the échelle-spectrograph PFES (mounted at the prime focus, 1K×1K CCD-chip, resolving power R = 15 000, Panchuk et al. 1998), the multi-mode échelle-spectrograph LYNX (Nasmyth-2 focus, 1K×1K CCD-chip, R = 30 000, Panchuk et al. 1999a), and the échelle-spectrograph NES (Nasmyth–2 focus, 2K×2K CCD-chip, R = 60 000, Panchuk et al. 1999b). The observing log is presented in Table 1. The cosmic ray traces were removed by median averaging of two subsequent spectra. A hollow cathode Th-Ar lamp was used for the wavelength calibration.

Table 1. Observing log for IRAS 01005+7910.

Date	Exposure time, s	Sp.range Å	Resolv. power, R	$\overline{S/N}$
06/07/2000	2 × 3200	4300–7800	15 000	100
13/07/2000	2 × 3200	4300–7800	15 000	180
09/11/2000	2 × 3200	4720–6320	30 000	120
03/01/2001	2 × 2400	4950–6600	15 000	220
11/08/2001	2 × 3200	5300–6680	30 000	100
02/12/2001	2 × 3600	4600–6070	60 000	75
25/01/2002	2 × 3600	3500–5070	60 000	40
04/02/2002	2 × 3600	4600–6070	60 000	55

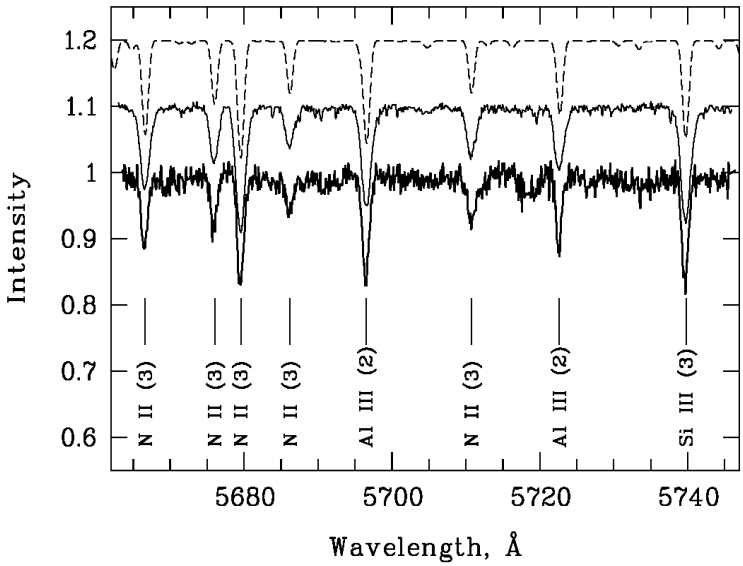

Fig.1. ***Nitrogen lines in the spectrum of IRAS 01005+7910 (thick line). The dashed line represents a synthetic spectrum for Teff = 21000 K, log g = 3.0 and et = 15 km s^{-1}. The spectrum of 9 Cep (thin line) is plotted between the theoretical one and that of IRAS 01005.***

First steps of the data reduction process (cosmic ray trace removal, background subtraction, and spectral order extraction) were done under the ECHELLE context of MIDAS (version 01FEB), while the final steps (normalization to the continuum level and radial velocity (V_r) and equivalent width measurements) were completed using a package DECH20 (Galazutdinov 1992).

3. Main results

3.1. The spectrum of IRAS 01005+7910

The optical spectrum of IRAS 01005 is a combination of the photospheric spectrum of a hot star and circumstellar emission lines. The line identification was completed using several line lists of Kilian & Nissen (1989), Parthasarathy et al. (2000), a multiplet table of Moore (1945) and our own experience in identification of spectra of related objects IRAS 18062+2410 (Arkhipova et al. 2001a) and V1853Cyg

(Arkhipova et al. 2001b). Refined line wavelengths, oscillator strengths and excitation potentials were taken from the data base VALD (Piskunov et al. 1995). Absorption lines of C II/III, N II, O II, Al III, Si III, and the Mg II line at λ4481 Å are present in the spectrum of IRAS 01005. Pure emission features were identified with Si II lines and forbidden lines of [Fe II]. Both emission and absorption components are detected in the hydrogen Balmer lines, the resonance lines of the Na I $D_{1,2}$ doublet, He I lines, and Fe III lines. We also found the Si II doublet λλ4128, 4131 Å in absorption with the equivalent widths of 60 and 70 mÅ, respectively. The absence of lines with low excitation potentials and those of neutral elements (except for those of H I, He I, and Na I) indicates that the star has a high $T_{\rm eff}$. The full list of identified emission and absorption lines in the spectrum of IRAS 01005 in the region 4300–7800 Å is presented in Table 2. Unidentified lines are denoted by "UN".

Our spectra of IRAS 01005 contain several diffuse interstellar bands. The most intense of them are the following: λ5780Å(W_λ = 100 mÅ), λ5797 Å (W_λ = 40 mÅ) and λ6613 Å (W_λ = 30 mÅ). Their $V_{\rm r} \sim -10$ km s^{-1} agree with the interstellar origin. The strength of the λ5780 Å band corresponds to the interstellar reddening E_{B-V} = 0.2 or A_V = 0.6 (Herbig 1993).

3.2. Spectral type and abundance calculation

In order to estimate the spectral type of IRAS 01005 we used a calibration for supergiants based on the line equivalent widths from Didelon (1982). Using only the lines without noticeable emission components (Mg II λ4481 Å, Si III λλ4553, 4575 Å and Si II λ4128 Å), we derived an average type of B 1.7 ± 0.5 which is in agreement with the abovementioned result of Hu (2001). We also compared the spectrum of IRAS 01005 with that of the normal supergiant 9 Cep (B2 Ib) and found them very similar (Fig. 1). While the strength of the nitrogen and oxygen lines in the spectrum of IRAS 01005 is in agreement with the estimated spectral type, the carbon lines are somewhat stronger (Fig. 2) suggesting its overabundance. The latter agrees with the object's carbon-rich IR spectrum.

We note here that these estimates are based on the spectral type criteria for population □ stars. Application of these criteria to stars with a possible metal deficiency and evolutionarily-altered abundances of light elements can insert significant systematic errors in the spectral classification. Nevertheless, the absence of He II and Si IV lines indicates that $T_{\rm eff} \leq 25\,000$ K, while the presence of He I lines in emission places a lower limit of $T_{\rm eff}$ at ~ 18 000−20 000 K (e.g., Miroshnichenko et al. 1998).

For an independent $T_{\rm eff}$ estimate, we compared the observed spectrum with a synthetic one, calculated from the Kurucz (1993) LTE models with the solar chemical composition. The best fit was obtained for $T_{\rm eff}$ = 21000K, microturbulent velocity ξ_t = 15 km s^{-1}, and surface gravity log g = 3.0 (see Figs. 1 and 2).

Overall, the spectrum of IRAS 01005 is very similar to that of a low-mass post-AGB star V1853 Cyg = LS II +34° 26 (B 1.5 Ia, García-Lario et al. 1997; Arkhipova et al. 2001a). For example, V 1853 Cyg exhibits a strong oxygen IR-triplet at λ7773 Å (W_λ = 0.95 Å), whose intensity increases with luminosity (Faraggiana et al. 1988). In the spectrum of IRAS 01005 this triplet has W_λ = 0.75 Å, confirming its high luminosity. However, we cannot estimate the latter due to a lack of hot stars with the measured strength of the triplet.

Since the spectrum of IRAS 01005 contains many absorption lines without visible emission components (see Table 2), we can estimate abundances of several chemical elements in its atmosphere. However, we have to keep in mind that both the model parameters and chemical composition, determined for such a hot and luminous star with the unstable and extended gaseous-dusty envelope in the framework of a static plane-parallel atmospheric model under the LTE approach, can be considered as a first approximation only.
All atomic parameters for the lines from Table 2 (oscillator strengths, damping constants, etc.) were taken from the VALD database (Piskunov et al. 1995). Note that virtually all the He I lines are distorted by emission components, therefore we were not able to estimate the He content.

Table 2. *Emission (e) and absorption (a) lines indentified in the spectrum of IRAS 01005+7910. V^1_r and V^2_r are the heliocentric V_r at two epochs (July 13, 2000 and December 2, 2001 respectively). W_λ is the equivalent width for the lines in the spectrum of July 13, 2000.*

λ_{lab} Å	Spec. (mult)	log(gf)		W_λ Å	V^1_r km s^{-1}	V^2_r km s^{-1}	λ_{lab} Å	Spec. (mult)	log(gf)		W_λ Å	V^1_r km s^{-1}	V^2_r km s^{-1}
4317.136	O II (2)	−0.386	a	0.107	−39		5073.903	Fe III (5)	−2.557	a	0.034	−40	
4319.625	O II (2)	−0.380	a	0.145	−46		5086.701	Fe III (5)	−2.590	a	0.032	−21	
4325.764	O II (2)	−1.099	a		blend		5127.463	Fe III (5)	−2.057	e	0.017	−72	−68
4325.993	C II (28)	−0.089	a		blend					a	0.027	−27	−23
4331.813	O II (41)	−0.090	a	0.027	−39		5133.121	C II (16)	0.107	a	0.062	−46	−27
4336.861	O II (2)	−0.762	a	0.078	−42		5143.497	C II (16)	−0.212	a	0.050	−49	
4340.462	H I (1)	−0.447	e	0.205	−43		5145.167	C II (16)	0.189	a	0.098	−54	−31
4345.558	O II (2)	−0.346	a	0.105	−50		5151.085	C II (16)	−0.179	a	0.038	−46	−36
4347.379	O II (16)	0.029	a	0.045	−48		5156.111	Fe III (5)	−2.018	e	0.025	−72	−66
4349.427	O II (2)	0.060	a	0.178	−49					a	0.029	−28	−22
4351.268	O II (16)	0.251	a	0.060	−43		5158.810	[FeII] (19F)		e	0.040	−58	−51
4359.340	[FeII] (7F)		e	0.040	−56		5197.577	Fe II (49)	−2.100	e	0.067	−32	−32
4366.893	O II (2)	−0.348	a	0.140	−53		5199	UN		e	0.005		
4387.929	He I (51)	−0.883	a	0.390	−41		5200	UN		e	0.040		
4411.364	C II (39)	0.918	a	0.036	−60		5206.650	O II (32)	−0.266	a	0.021	−35	
4414.900	O II (5)	0.172	a	0.180	−53		5219	UN		a	0.022		
4416.980	O II (5)	−0.077	a	0.120	−46		5227.830	Fe III	−0.055	a	0.017	−45	
4437.551	He I (50)	−2.034	a	0.094	−41		5261.620	[FeII] (19F)		e	0.015	−59	
4447.030	N II (55)	0.285	a	0.088	−49		5273.380	[FeII] (18F)		e	0.010	−62	−52
4452.380	O II (5)	−0.789	a	0.044	−41		5357	UN		e	0.065		
4471.485	He I (14)	0.053	a	0.430	−26		5454.214	N II (29)	−0.827	a	0.042	−48	
4481.207	Mg II(4)	0.985	a	0.190	−33		5463	UN		a	0.035		
4512.565	Al III (3)	0.410	a	0.026	−41		5495.653	N II (29)	−0.266	a	0.036	−47	
4529.164	Al III (3)	0.706	a	0.072	−47		5639	UN		a	0.050		
4552.622	Si III (2)	0.181	a	0.274	−51		5646	UN		a	0.035		
4567.840	Si III (2)	−0.039	a	0.220	−53	−29	5662.459	C II (15)	−0.249	a	0.025	−44	
4574.757	Si III (2)	−0.509	a	0.110	−51		5666.627	N II (3)	−0.045	a	0.118	−42	−27
4590.974	O II (15)	0.350	a	0.088	−50	−32	5676.015	N II (3)	−0.368	a	0.106	−37	−30
4596.160	O II (15)	0.225	a	0.075	−49		5679.554	N II (3)	0.250	a	0.200	−33	−31
4601.481	N II (5)	−0.428	a	0.035	−35		5686.212	N II (3)	−0.549	a	0.049	−35	−11
4607.149	N II (5)	−0.507	a	0.044	−46		5696.604	Al III (2)	0.230	a	0.168	−46	−34
4609.473	O II (93)	0.729	a	0.042	−51		5710.766	N II (3)	−0.518	a	0.074	−43	−25
4613.670	O II (92)	−1.040	a		blend		5722.730	Al III (2)	−0.070	a	0.123	−46	−31
4613.868	N II (5)	−0.665	a		weak		5730.660	N II (3)	−1.704	a	0.020	−40	
4619.249	C II	1.142	a	0.014	−49		5739.734	Si III (4)	−0.160	a	0.220	−47	−34
4621.241	O II (92)	−1.150	a		blend		5780.410	DIB		a	0.100	−10	
4621.396	N II (5)	−0.514	a	0.012	−35		5797.030	DIB		a	0.040	−8	
4630.543	N II (5)	0.094	a	0.106	−40	−28	5833.938	Fe III (114)	0.616	a	0.037	−40	
4638.851	O II (1)	−0.332	a	0.107	−50	−27	5875.661	He I (11)	0.740	e		−39	−22
4641.810	O II (1)	0.054	a	0.215	−53	−29				a		8	−35
4643.090	N II (5)	−0.359	a	0.052	−40	−28	5889.951	Na I (1)	0.117	a	0.160		−72
4647.419	C III (1)	0.070	a	0.070	−50	−34				a	0.070	−67	−66
4649.138	O II (1)	0.308	a	0.292	−47	−30				a	0.080		−52
4650.838	O II (1)	−0.361	a	0.160	−50	−29				a	0.125		−28
4651.018	C III (1)	−0.432	a		blend					a	0.330	−17	−11
4661.635	O II (1)	−0.278	a	0.135	−47	−30	5895.924	Na I (1)	−0.184	a	0.125		−73
4673.732	O II (1)	−1.089	a	0.043	−41					a	0.055	−68	−65
4676.231	O II (1)	−0.395	a	0.118	−44	−33				a	0.060		−52
4696.356	O II (1)	−1.380	a	0.009	−45					a	0.090		−28
4699.215	O II (25)	0.270	a	0.047	−54					a	0.300	−16	−10
4703.209	O II (40)	0.538	a	0.013	−64		5957.559	Si II (4)	−0.301	e	0.026	−49	−54
4705.343	O II (25)	0.476	a	0.062	−51		5978.930	Si II (4)	0.004	e	0.090	−44	−53
4710.012	O II (24)	−0.226	a	0.019	−48		6195.990	DIB		a	0.030	−10	
4713.171	He I (13)	−0.976	a	0.140	−28	−22	6203.060	DIB		a	0.050	−19	
4803.287	N II (20)	−0.113	a	0.023	−53		6347.109	Si II (2)	0.297	e	0.171	−57	
4813.333	Si III (9)	0.850	a		weak		6371.371	Si II (2)	−0.003	e	0.065	−54	
4814.550	[FeII] (20F)		e	0.025	−56	−52	6379.616	N II (2)	−0.951	a	0.041	−32	
4819.688	Si III (9)	0.998	a	0.060	−54		6402.246	Ne I (1)	0.360	a	0.057	−37	
4828.957	Si III (9)	1.111	a	0.060	−51		6548.100	[N I] (1F)		e	0.050	−55	
4856.594	O II (29)	−0.583	a	0.060	−47		6562.797	H I (1)	0.710	e	13.0	−35	
4861.323	H I (1)	−0.020	e	1.80	−45	−29	6578.053	C II (2)	−0.026	a	0.258	−30	
4905.350	[FeII] (20F)		e	0.006	−58		6582.882	C II (2)	−0.328	a	0.057	−31	
4906.830	O II (28)	−0.160	a	0.037	−58		6583.600	[N I] (1F)		e		bl.	
4921.931	He I (48)	−0.435	a	0.470	−32	−42	6605	UN		e	0.110		
4924.525	O II (28)	0.074	a	0.037	−53		6613.630	DIB		a	0.030	−16	
4994.367	N II (24)	−0.069	a	0.016	−50		6678.154	He I (46)	0.329	a	0.258	−15	
5001.339	N II (19)	0.661	a	0.110	−48	−33	6721.384	O I (4)	−0.609	a	0.057	−48	
5005.154	N II (19)	0.592	a	0.094	−51	−33	6779.939	C II (14)	0.024	a		bl.	
5007.333	N II (24)	0.171	a	0.042	−48	−30	6780.599	C II (14)	−0.377	a		bl.	
5010.622	N II (4)	−0.606	a	0.045	−42	−29	6783.908	C II (14)	0.304	a	0.054	−43	
5012.032	N II (64)	0.136	a	0.009	−58		6787.207	C II (14)	−0.378	a	0.016	weak	
5015.678	He I (4)	−0.820	e		−67	−48	6791.466	C II (14)	−0.271	a	0.025	weak	
			a		−23	−14	6798.104	C II (14)	−1.077	a	0.	weak	
5041.024	Si II (5)	0.291	e	0.018	−55	−58	6800.683	C II (14)	−0.345	a	0.020	weak	
5044.356	C II (35)	−0.500	a		blend		7065.246	He I (10)	−0.205	e		−58	
5045.103	N II (4)	−0.407	a	0.082	−55	−33				a		11	
5047.117	C II (35)	−1.000	a		blend		7771.941	O I (1)	0.369	a	0.334	−26	
5047.738	He I (47)	−1.602	a	0.110	−34	−28	7774.161	O I (1)	0.223	a	0.263	−25	
5056.017	Si II (5)	0.639	e	0.090	−62	−53	7775.390	O I (1)	0.001	a	0.150	−28	

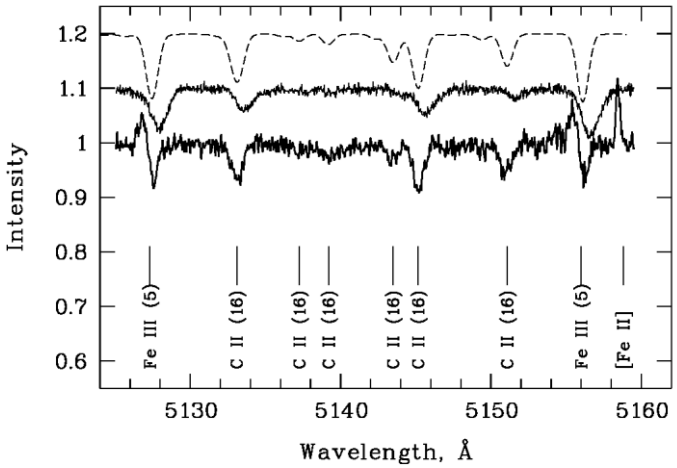

Fig. 2. ***Carbon lines in the spectrum of IRAS 01005+7910 (thick line). Other lines have the same meaning as in Fig. 1.***

The chemical abundances were calculated using the Kurucz (1993) models and Kurucz's WIDTH9 program. The effective temperature ($T_{\rm eff}$ = 21500 ± 500 K) and the surface gravity (log g = 3.0 ± 0.3) values were improved by using the criterion of the Si II/Si III ionization balance, i.e. equality of the Si II and Si III abundances. The estimated uncertainties in the abundances caused by the errors in $T_{\rm eff}$ and log g are equal to ±0.2 dex, which are similar to those due to the errors of the equivalent widths. A good agreement of the abundances derived for the pair C II/C III supports the above model atmosphere parameters. In order to estimate the microturbulent velocity ξ_t, we used the numerous well-measured O II absorption lines and found that such a ξ_t value produced a zero slope in a diagram of log abundances calculated for individual O II lines versus equivalent widths. Formal application of the generally adopted method leads to a very large value of ξ_t = 45 ± 5 km s^{-1}. It is evident that the supersonic value of ξ_t is mainly caused by use of a plane-parallel static atmosphere model approximation for a high-luminosity and high-temperature star with an unstable atmosphere. Takeda (1992) showed that the microturbulent velocity suddenly grows when the atmosphere becomes unstable, because the radiation force is larger than the gravitational force. Such unrealistically large microturbulent velocities, obtained under the LTE–approach, is a well-known fact in hot star spectra simulations (Takeda 1977). Gies & Lambert (1992) showed that, taking into account deviations from the LTE approximation, the microturbulent velocity can be reduced from 25–30 to 8–11 km s^{-1}. To reduce systematic errors and derive more realistic chemical abundances, we did not take into account all the strong lines with $W_\lambda \geq$ 80 mÅ, since the weak lines are practically independent of the microturbulent velocity. A typical value of ξ_t = 15 ± 5 km s^{-1} for high-luminosity hot stars (Gies & Lambert 1992; Parthsarathy et al. 2000) within the LTE-approach was adopted in our calculations.

To illustrate the role of non-LTE effects for the IRAS 01005 spectrum we calculated an oxygen abundance from the lines of both ions and neutral atoms. It is well known that the lines of the oxygen IR-triplet at λ7773 Å are very sensitive to non-LTE effects. Using the equivalent widths of these lines from Table 2 we obtained ε(O I) = 9.49, while a lower value of ε(O II) = 8.24 was derived from the weak O II lines.

The average chemical abundances for different species are presented in Table 3. The abundances are given on the usual scale, ε(X) = n(X)/n(H) with log ε(H) = 12. The chemical composition for a normal supergiant 9 Cep (Gies & Lambert 1992) is given for comparison.

As follows from Table 3, the atmospheric abundances of all the elements found for IRAS 01005 and for a normal super-giant 9 Cep are different. The iron content [Fe/H]$_\odot$ = −0.31 of IRAS 01005 is slightly smaller relative to the solar one, while it is larger for 9 Cep ([Fe/H] $_\odot$ = +0.18). The abundances of such metals as Mg, Al, and Si show the same feature in both objects. As follows from the results by Gies & Lambert (1992), a chemical abundance pattern in the case of 9 Cep agrees with the evolutionary stage of a massive supergiant: carbon is under abundant in its metal-rich atmosphere, contaminated by the CN-cycle products. The CNO-group behaviour in the IRAS 01005 atmosphere (the carbon abundance is enhanced relative to the solar one, [C/Fe] $_\odot$ = +0.08, while the oxygen content is deficient, [O/Fe] $_\odot$ = −0.32) is opposite to that of 9

Cep. These differences in the chemical abundance picture allow us to rule out a hypothesis that IRAS 01005 is a normal supergiant.

We note here that the main spectral peculiarities, the atmospheric parameters $T_{\rm eff}$ = 21500 K, log g = 3.0, and the atmospheric abundances of IRAS 01005 are similar to those of the post-AGB object IRAS 18062+2410, whose high-resolution spectra were studied by Arkhipova et al. (2001a) and Parthasarathy et al. (2000). The most remarkable difference between IRAS 01005 and IRAS 18062+2410 is the behaviour of the CNO abundances (Table 3). For IRAS 18062+2410, the N– and O–abundances are similar to the metallicity at a strong C–deficiency. For IRAS 01005 we see a different picture: the C– and N–abundances follow the iron content at a large oxygen deficiency. The carbon/oxygen ratio is C/O < 1 for IRAS 18062+2410 while for IRAS 01005 the ratio C/O > 1 is in agreement with details in its IR–spectrum (Hrivnak et al. 2000, see Sect. 1). Therefore we confirmed a result by Hrivnak et al. (2000) that the central star of IRAS 01005 belongs to the group of carbon-rich PPNe.

Table 3. ***The chemical composition of IRAS 01005, log ε(X) (for log ε(H) = 12.0). n refers to the number of lines used, and a- is the uncertainty derived from the measurements of individual lines. Atmospheric parameters (T_{eff} (K), log g, ξt (km s^{-1})) of the stars are given below their names. The element abundances for the solar photosphere are taken from Grevesse et al. (1996).***

Sun		IRAS 18062+2410 [1] 22 000, 3.0, 15		9 Cep [2] 19 040, 2.61, 28.9	IRAS 01005+7910 21 500, 3.0, 15			
X	log ϵ(X)	log ϵ(X)	X	log ϵ(X)	log ϵ(X)	*n*	σ	$[X/H]_\odot$
C	8.55	6.95	C II	8.12	8.32	6	0.12	−0.23
			C III		8.42	1		−0.13
N	7.97	7.27	N II	8.03	7.70	10	0.25	−0.27
O	8.87	8.27	O II	8.66	8.24	12	0.21	−0.63
Mg	7.58	7.08	Mg II		7.44[3]	1		−0.13
Al	6.47	5.87	Al III		5.82	2		−0.65
Si	7.55	6.75	Si II	6.87	7.41	2		−0.14
			Si III		7.40	5	0.20	−0.15
Fe	7.50	6.90	Fe III	7.68	7.19	4	0.20	−0.31

[1] Results from Parthasarathy et al. (2000) are recalculated using the solar abundances from Col. 2.
[2] From Gies & Lambert (1992).
[3] The Mg abundance may be overestimated since it was derived from strong (W_λ = 190 mÅ) line.

3.3. Spectral variability

In the spectra obtained in 2000, the hydrogen Balmer lines Hα, Hβ and Hγ have asymmetric single-peaked emission profiles (Fig. 3) with a maximum intensity at a $V_{\rm r}$ of −40km s^{-1}. The intensity of the blue wing decreases faster at low velocities than that of the red wing, while the situation is reversed at velocities more than 40 km s^{-1} from the line maximum. Such a profile can be a combination of two emission components with different intensities and a component due to self-absorption. In 2001 the Hα and Hβ profile shape became double-peaked with the intensities, which differ by an order of magnitude.

The He I line profiles vary from straight to inverse P Cyg-type through almost pure emission or absorption (Fig. 3). Furthermore, in the spectrum obtained on December 02, 2001 with R = 60 000 a straight P Cyg-type profile of the λ5876 Å line and an inverse P Cyg-type profile of the λ5016 Å line are seen together. At the same time, in this spectrum the He I line at λ4922 Å, which does not show emission wings, is split into two absorption components, as if a weak emission in the core is present. Finally, on July 06, 2000 the λ4922 Å and λ6678 Å lines have inverse P Cyg-type profiles with the emission and absorption components at −75 and −27 km s^{-1}, respectively. However, on July 13, 2000 noticeable emission components are absent in both lines.

The $V_{\rm r}$ behaviour of individual lines is more complicated. The $V_{\rm r}$ of both the absorption and emission lines correlate with the oscillator strengths (Fig. 4): the stronger lines have more negative velocities. This is more likely a result of a velocity gradient in the expanding envelope and atmosphere of the supergiant.

Furthermore, the slope of the linear relationship varies from one spectrum to another (Fig. 4). The systemic velocity we define as a limiting velocity of the lines with small oscillator strengths. For all our spectra this limit is -23 ± 3 km s^{-1}.

In Table 4 we show the heliocentric V_r derived from absorption and emission lines and/or their components at different epochs. A typical uncertainty of the V_r measurements for a single line is about 1 km s^{-1} for the spectrometer NES, 2 km s^{-1} for LYNX, and 4 km s^{-1} for PFES. A significant shift (-15 km s^{-1}) in most of the absorption line V_r (except for those of Fe III) occurred in December 2001. This phenomenon may be due to changes in the star's atmospheric structure, which may also cause the disappearance of the Hβ line absorption component. Pulsations as a mechanism, responsible for similar V_r variations, was suggested by García-Lario et al. (1997) for V 1853 Cyg. Our present time coverage does not allow us to comment on other possible reasons for it, such as orbital motion in a binary system.

In Fig. 5 the Na I resonance doublet profiles, obtained with the $R = 60\,000$ on two different dates, are shown. We were able to distinguish five absorption components with velocities of -11, -28, -52, -65, and -73 km s^{-1}. In addition, the absorption profile of the λ5890 Å line in the spectrum of December 2, 2001 is superseded on a broad high-velocity emission component, whose width is the same as those of the hydrogen line emission components. In the other spectrum there are no noticeable emission components. The first and the strongest absorption component has a V_r of -3 km s^{-1} with respect to local standard of rest, and is most likely interstellar. The radio observations of the CO emission (Grenier et al. 1989) and those of the interstellar Na I lines for nearby stars in the direction of IRAS 01005 (e.g., Welty et al. 1994) give the LSR velocity for the interstellar medium from -8 to $+10$ km s^{-1}.

The next Na I component in the spectrum of IRAS 01005 (at -28 km s^{-1}) is located very close to the systemic velocity. It may be formed in the outer, slowest (V_{exp} & 5–10kms^{-1}), and optically thin part of the circumstellar envelope. The three remaining components may arise either in more rapidly expanding shells or in the interstellar medium.

4. Discussion

The spectral features mentioned above led us to the following suggestions. The system of IRAS 01005 contains a high-luminosity early-B type star surrounded by a gaseous envelope. The transformation of the He I line profiles from inverse (in 2000) to straight (in 2001) P Cyg-type is suggestive of a change from accretion to outflow in the inner parts of the envelope. The increasing separation between the emission components of the Ha line observed simultaneously supports the outflow hypothesis. The co-existence of the straight and inverse P Cyg-type profiles in different He I lines in one spectrum suggests that accretion and outflow can be present at the same time, however probably in different parts of the envelope. The difference in the profile shapes of the Balmer and He I lines may be due to a more spherical zone of the He I line formation, as it has been suggested for an LBV candidate MWC 314 (Frémat et al. 1998).

The presence of the relation between the line velocity and the oscillator strength may be due to the velocity gradient in the unstable atmosphere of IRAS 01005. Phases of atmosphere instability from time to time alternate with phases of a relative quiescence, characterized by a low or negligible velocity gradient (Fig. 4).

Given a high luminosity, the star should be distant. From his optical photometry, Hu (2001) suggested that the interstellar extinction $A_V = 1.2$, while not attempting a distance estimate, as IRAS 01005 is peculiar. Indeed, both luminosity and kinematic distance calibrations are mostly based on the galactic disk stars, while IRAS 01005 most likely belongs to the halo. Our result for A_V (Sect. 3.1) might imply that part of the extinction is circumstellar.

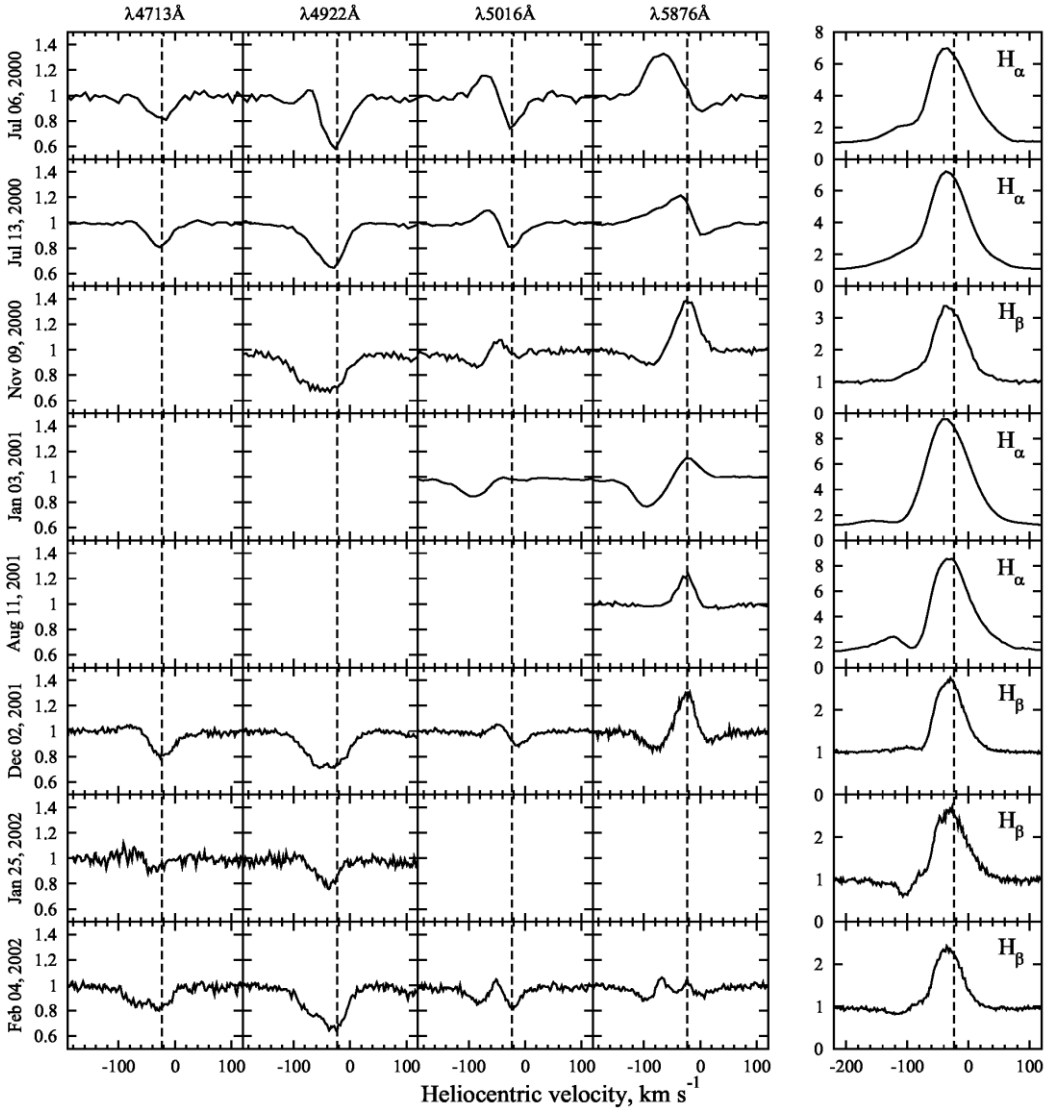

Fig. 3. *The He I and Balmer line profile variations. The suggested systemic velocity −23 km s^{-1} is shown by vertical dashed lines.*

Table 4. *Heliocentric V_r (km s^{-1}) in the spectrum of IRAS 01005. The number of lines used for the measurements is given in parentheses.*

Ion (Mult.)	Jul. 2000	Nov. 2000	Aug. 2001	Dec. 2001	Jan. 2002	Feb. 2002
			Absorption lines			
C II (16)	−49 (4)			−31 (3)		−50 (3)
N II (3)	−38 (6)	−50 (5)	−41 (5)	−25 (5)		−43 (5)
O II (1)	−47 (8)			−30 (6)	−41 (7)	−47 (7)
Al III (2)	−46 (2)	−51 (2)	−46 (2)	−33 (2)		−47 (2)
Si III (2,4)	−50 (4)	−48 (1)	−45 (1)	−32 (2)	−39 (3)	−43 (1)
Fe III (5)	−27 (2)			−23 (2)		−23 (1)
Hα			−92			
Hβ				−84	−105, −75	−118, −80
Hγ	−179				−103, −73	
			Emission lines			
[FeII] (7,18–20)	−58 (6)			−51 (3)	−51 (1)	−53 (3)
Fe III (5)	−72 (2)			−67 (2)		
Si II (2,4,5)	−54 (6)	−49 (3)	−55 (4)	−56 (4)		−50 (4)
Hα	−35		−32, −124			
Hβ	−45	−34		−100, −30	−32	−35
Hγ	−43				−39	

Let us try to estimate the luminosity and distance of IRAS 01005 by using the values $T_{\rm eff}$ = 21500 K and log g = 3.0 we obtained. As follows from the locus of likely post–AGB stars in the log g vs. $T_{\rm e}$ff plane (Fig. 3 from Schönberner & Blöcker 1993), we can adopt a mass of the object of $M \approx 0.57 \pm 0.05\ M\odot$. According to theoretical post-AGB evolutionary tracks (Blöcker 1995), such an object would have a luminosity of $\log(L/L\odot) = 3.6$ ($M_{\rm bol} = -4.3$). From the observed V = 11.2mag (Hu 2001) and the interstellar (and circumstellar) extinction A_V = 1.2mag, we have the dereddened V_0 = 10 mag and, accepting the bolometric correction $BC = -2$ mag, we obtain $V_0 - M_V$ = 12.3 mag, that corresponds to a distance of ~3 kpc. Taking into account the uncertainties in the effective temperature and surface gravity (see Sect. 3.2), we estimate an error of the distance determination to be about 20%. Such a distance is consistent with the presence of the sodium D-lines absorption components at $V_{\rm r} = -52$ km s^{-1} that may be due to the interstellar material within the Perseus arm (Münch 1957). The interstellar origin of the higher-velocity components (see Fig. 5) requires a larger distance toward the object, which would make it more luminous and more rapidly evolving along the post-AGB track. Since there is no evidence of rapid evolution, one can suggest that these components were formed in the circumstellar envelope ejected during the AGB-phase.

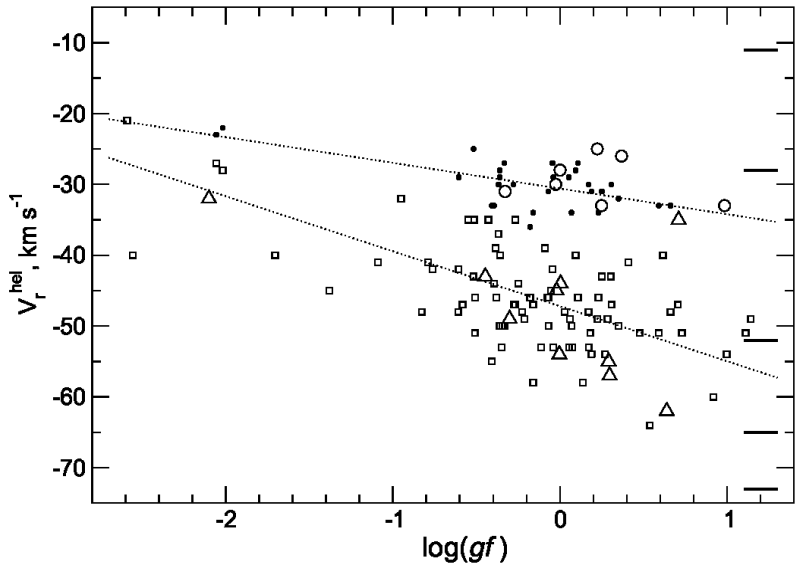

Fig. 4. ***Relations between the heliocentric V_r of the absorption lines and oscillator strengths at two epochs July 13, 2000 (open squares) and December 02, 2001 (dots) (see Table 2). The dotted lines show the linear fits to the relations. The emission lines in the July 2000 spectrum (open triangles) show the same distribution as the absorption lines. The open circles denote the group of the strong absorption lines in the July 2000 spectrum (O I triplet λ7773 Å, Mg II λ4481 Å, C II λλ6578, 6583 Å and N II λ5680 Å). The velocities of the Na I $D_{1,2}$ line components are shown by thick horisontal lines.***

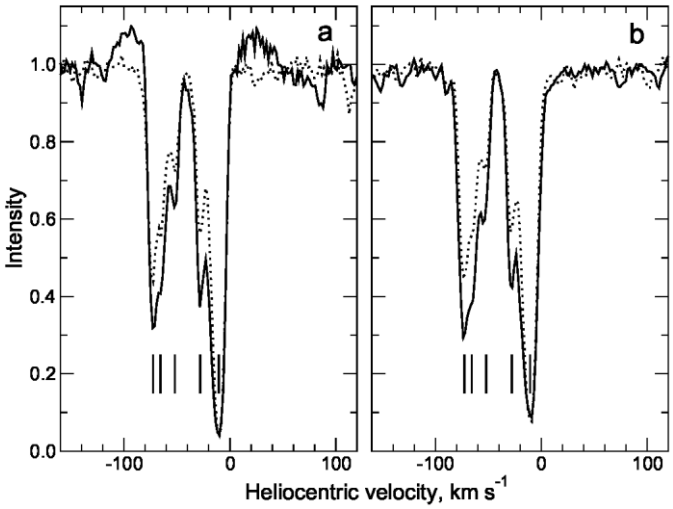

Fig. 5. ***The Na I D_1 (dotted) and D_2 (solid) line profiles in high resolution spectra of Dec. 2001 (a) and Feb. 2002 (b).***

The reduced metallicity of IRAS 01005 $[Fe/H]_\odot = -0.31$ in combination with the altered CNO-abundances (C/O > 1) and the high galactic latitude, suggests that it is a hot post– AGB star. If its luminosity and, hence, mass are large enough, the star's T_{eff} will increase quickly (Blöcker 1995). As a result, one can expect an increase of the emission-line strengths in the object's spectrum, because in comparison with other early-type PPNe (OY Gem and IRAS 18062+2410), IRAS 01005 shows a relatively weak emission-line spectrum. Alternatively, the latter might imply that its gaseous envelope is compact, being limited by the presence of a companion star. Another indication for binarity can be the envelope's asphericity (inferred from the emission line profiles). Therefore, further spectroscopic monitoring of IRAS 01005 is highly desirable to further constrain its properties.

5. Conclusions

We accomplished the first detailed indentification of the observed features in the high-resolution optical spectrum of an optical counterpart of the PPN candidate IRAS 01005. The absorption lines of C II/III, N II, O II, Al III, Si II/III, and the Mg II λ4481 Å line, as well as emission lines of Si II and [Fe II] were found in the spectrum. Both emission and absorption components are present in the hydrogen Balmer lines, in the resonance Na I $D_{1,2}$ lines, and in the He I and Fe III lines. A significant variability of the optical spectrum was detected: the He I lines change their profiles from straight to inverse P Cyg-type on a timescale of days-months.

A high effective temperature T_{eff} = 21500 K, a low surface gravity log g = 3.0, and a reduced metallicity of IRAS 01005 ($[Fe/H]_\odot = -0.31$) in combination with the altered atmospheric CNO–abundances (C/O > 1) and a high galactic latitude, confirm the evolutionary state of a hot post-AGB C-rich star.

We suggest that IRAS 01005 is a high-luminosity $\log(L/L_\odot) = 3.6$ early-B type post-AGB star at a distance of ~3 kpc, surrounded by a non-spherical gaseous envelope with both observable accretion and outflow. The envelope geometry and weakness of the emission-line spectrum may indicate binarity of the system.

Acknowledgements. We are much indebted to the anonymous referee, who stimulated the analysis of the chemical composition of IRAS 01005. This work was supported in part by Russian Foundation for Basic Research (project No. 02–02–16085). The research described in this publication was made possible in part by Award No. RP1–2264 of the U.S. Civilian Research & Development Foundation for the Independent States of the Former Soviet Union (CRDF). This research has made use of the SIMBAD database operated at CDS (Strasbourg, France) and of the VALD database operated at Vienna.

References

Arkhipova, V. P., Klochkova, V. G., & Sokol, G. V. 2001, Astron. Lett., 27,99
Arkhipova, V. P., Ikonnikova, N. P., Noskova, R. I., et al. 2001, Astron. Lett., 27, 719
Blöcker, T. 1995, A&A, 299, 755
Decin, L., Van Winckel, H., Waelkens, C., & Bakker, E. J. 1998, A&A, 332,928
Didelon, P. 1982, A&AS, 50,199
Faraggiana, R., Gerbaldi, M., van't Veer, C., & Floquet, M. 1988, A&A, 201, 259
Frémat, Y., Miroshnichenko, A. S., & Houziaux, L. 1998, in B [e] stars,
ed. A.-M. Hubert, & C. Jaschek (Kluwer Acad. Publ.), 97
Galazutdinov, G. A. 1992, Preprint of the Spec. Astrophys. Obs., No. 92
García-Lario, P., Parthasarathy, M., de Martino, D., et al. 1997, A&A, 326, 1103
Gies, D. R., & Lambert, L. 1992, ApJ, 387, 673
Grenier, I. A., Lebrun, F., Arnaud, M., Dame, T. M., & Thaddeus, P. 1989, ApJ, 347, 231
Grevesse, N., Noels, A., & Sauval, A. J. 1996, ASP Conf. Ser., 99,117 Herbig, G. H. 1993, ApJ, 407, 142
Hrivnak, B., Volk, K., & Kwok, S. 2000, ApJ, 535, 275
Hu, J. Y. 2001, in Post-AGB Objects as a Phase of Stellar Evolution, Proc. of the Torun Workshop, ed. R. Szczerba, & S. K. Górny (Kluwer Acad. Publ.), 317
Kilian, J., & Nissen, P. E. 1989, A&AS, 80, 255
Klochkova, V. G. 1998, Bull. Spec. Astrophys. Obs., 44, 5
Kurucz, R. L. 1993, Smithsonian Astron. Obs., CD ROM, No. 19

Lambert, D. L., Hinkle, K. H., & Luck, R. E. 1988, ApJ, 333, 917 Lewis, B. M. 1989, ApJ, 338, 234
Likkel, L. 1989, ApJ, 344, 350
Likkel, L., Forveille, T., Omont, A., & Morris, M. 1991, A&A, 246, 153
Miroshnichenko, A. S., Fremat, I., Houziaux, L., et al. 1998, A&AS, 131,469
Moore, C. E. 1945, A multiplet table of astrophysical interest
Münch, G. 1957, ApJ, 125, 42
Omont, A., Loup, C., Forveille, T., et al. 1993, A&A, 267, 515
Panchuk, V. E., Najdenov, I. D., Klochkova, V. G., et al. 1998, Bull. Spec. Astrophys. Obs., 44, 127
Panchuk, V. E., Klochkova, V. G., Najdenov, I. D., et al. 1999a, Preprint of the Spec. Astrophys. Obs., No. 139
Panchuk, V. E., Klochkova, V. G., & Najdenov, I. D. 1999b, Preprint of the Spec. Astrophys. Obs., No. 135
Parthasarathy, M., & Pottasch, S. R. 1989, A&A, 225, 521
Parthasarathy, M., García-Lario, P., Sivarani, T., Manchado, A., & Sanz Fernandez de Cordoba, L. 2000, A&A, 357, 241
Piskunov, N. E., Kupka, F., & Ryabchikova, T. A. 1995, A&AS, 112, 525
Schönberner, D., & Blöcker, T. 1993, ASP Conf. Ser., 45, 337
Takeda, M. 1977, PASJ, 29, 439
Takeda, M. 1992, PASJ, 44, 309
Van der Veen, V. E. C. J., & Habing, H. J. 1988, A&A, 194, 125
Van Winckel, H. 2001, Ap&SS, 275,159
Van Winckel, H., Waelkens, C., & Waters, L. B. F. M. 1995, A&A, 239, L25
Welty, D. E., Hobbs, L. M., & Kulkarni, V. P. 1994, A&AS, 100, 107